www.czasopisma.pan.pl PAN POLSKA AKADEMIA NAUK www.journals.pan.pl

Arch. Metall. Mater. **66** (2021), 3, 789-793

DOI: 10.24425/amm.2021.136381

YURI KIM[1], HOSEONG RHEE[1], SI YOUNG CHANG[1*]

MICROSTRUCTURAL CHARACTERISTICS OF Ti-Al-Dy ALLOY PRODUCED BY HIGH ENERGY BALL MILLING

In this study, the alloying of Ti, Al and Dy powders by high energy ball milling, and the spark plasma sintering (SPS) characteristics of as milled powders have been investigated based on the observation of microstructure. Pure Ti, 6wt% Al and 4wt% Dy powders were mixed and milled with zirconia balls at 600 ~ 1000 rpm for 3h in an Ar gas. The initial sizes of Ti, Al and Dy powders were approximately 20, 40, and 200 μm, respectively. With increasing the milling speed from 600 to 1000 rpm, the size of mixing powders reduced from 120 to 15 μm. On the other hand, from XRD results of powders milled at higher speeds than 700rpm, the peaks of Ti_3Al and AlDy phases were identified, indicating the successful alloying. Therefore, the powders milled at 800 rpm have been employed for the SPS under the applied pressure of 50 MPa at 1373K for 15 min. In the SPSed sample, the Al_3Dy and two ternary Ti-Al-Dy phases were newly detected, while the peak of AlDy phase disappeared. The SPSed Ti-6Al-4Dy alloy revealed high relative density and micro-hardness of approximately 99% and 950Hv, respectively.

Keywords: High energy ball milling, Ti-Al-Dy powders, SPS, Microstructure, Micro-hardness

1. Introduction

Ti alloys have been recognized as very attractive materials for power generation, aerospace, automobile and biomedical industries because of their high specific strength, good creep and fatigue properties and excellent corrosion resistance and high biocompatability [1-4]. However, their low ductility and toughness at room temperatures prevent further application in engineering industry, and a low elastic modulus has been demanded for applications as medical implants. Guo et al. [5] have reported that Nb and Ta are suitable alloying elements to reduce the modulus. According to previous study [6], in addition, the addition of alloying elements such as V and rare earth elements is significantly effective for improving the low ductility. Recently, among rare earth elements, Dy could be easily extracted in large quantities from (Nd,Dy)FeB magnets waste [7,8]. Therefore, Dy has a potential as an alloying element for Ti alloys. However, the effect of Dy on microstructure and mechanical properties of Ti alloys has been well unknown. On the other hand, such Ti alloys have been generally produced by arc melting and powder metallurgy processing due to their high melting temperature. Among powder metallurgy processing, in particular, high energy ball milling is an effective method currently used to obtain not only amorphous phase or nanocrystalline structure in inorganic materials synthesis [9,10] but alloying in metallic materials [11-13]. Additionally, the spark plasma sintering (SPS) method has been employed for new materials, such as fine ceramics [14,15], nano phase materials [16], magnetic materials [17] and ferrous materials [18], because rapid heating rate, short holding time and low temperature during SPS lead to fine microstructure, high sintering density and easy manipulation compared to other conventional sintering methods [19,20]. Accordingly, it is of interest to apply the high energy ball milling and subsequently SPS for Ti alloys with Dy. The object in this study was to investigate the alloying of Ti-6wt% Al-4wt% Dy by the high energy ball milling and subsequently SPS based on the microstructural characteristics of as milled powders and as SPSed sample.

2. Experimental

Pure Ti, Al and Dy powders with a weight ratio of 90:6:4 were charged with zirconia ball into jars for high energy ball milling. The ball milling was conducted at various milling rates of 600 ~ 1000 rpm for 3 h under Ar atmosphere. The milled powders were collected in the glove box filled with argon gas,

[1] KOREA AEROSPACE UNIVERSITY, DEPARTMENT OF MATERIALS SCIENCE AND ENGINEERING, GOYANG 10540, KOREA

* Corresponding author: sychang@kau.ac.kr

and were subsequently subjected to spark plasma sintering (SPS) at 1373K for 15 min with graphite mold under the applied pressure of 50 MPa and argon atmosphere. The microstructures of powders and as sintered sample were observed by using a scanning electron microscope (SEM), and the mean size and shape factor (= $4\pi A/P^2$, where A is area and P is perimeter of powder) of powders were measured by an image analysis. The component and phase analyses in as milled powders and as sintered sample were conducted by an energy dispersive spectroscope (EDS) and an X-ray diffractometer (XRD). The relative density of as sintered sample was obtained by an Archimedes method. Vickers micro-hardness test was carried out under a load of 1 kg for 5 sec.

3. Results and discussion

Figure 1 shows the SEM photographs of initial Ti, Al, and Dy powders employed in this study. The initial Ti and Dy powders are irregular in shape, whereas the Al powder shows round typed shape. The initial sizes of Ti, Al and Dy powders are approximately 20, 40 and 200 μm, respectively. The EDS analysis of Ti-Al-Dy mixing powders milled at 600 rpm and SEM photographs of as milled Ti-Al-Dy mixing powders with increasing the milling rate are shown in Fig. 2 and 3, respectively. As shown in Fig. 2, the initial Ti, Al and Dy powders are well mixed by high energy ball milling and the mixing powders become round in shape. As the milling time increases, the mixing powders become obviously smaller. The mean size, shape factor and size distribution of mixing powders obtained from Fig. 3 are quantitatively plotted in Fig. 4. With increasing the milling rate from 600 to 100 rpm, the mean size of mixing powders is reduced from approximately 120 to 15 μm, and the shape factor increases to approximately 0.9, indicating that the mixing powders are almost sphere. The size distribution peak of mixing powders moves to the left with increasing the milling rate and is particularly in between 10 and 20 μm after milling at 1000 rpm. The highest number peaks well correspond to the mean size of mixing powders.

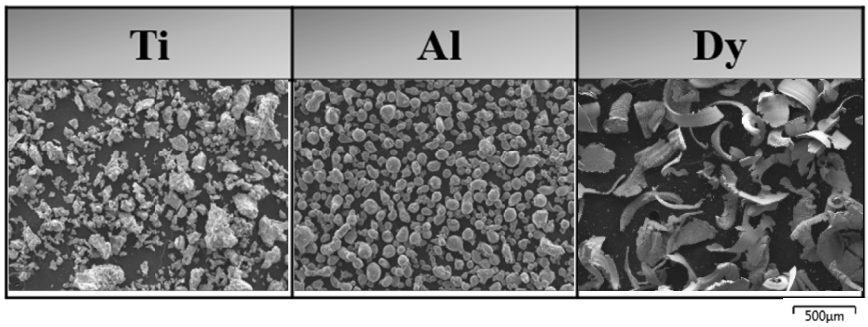

Fig. 1. SEM images showing initial Ti, Al and Dy powders

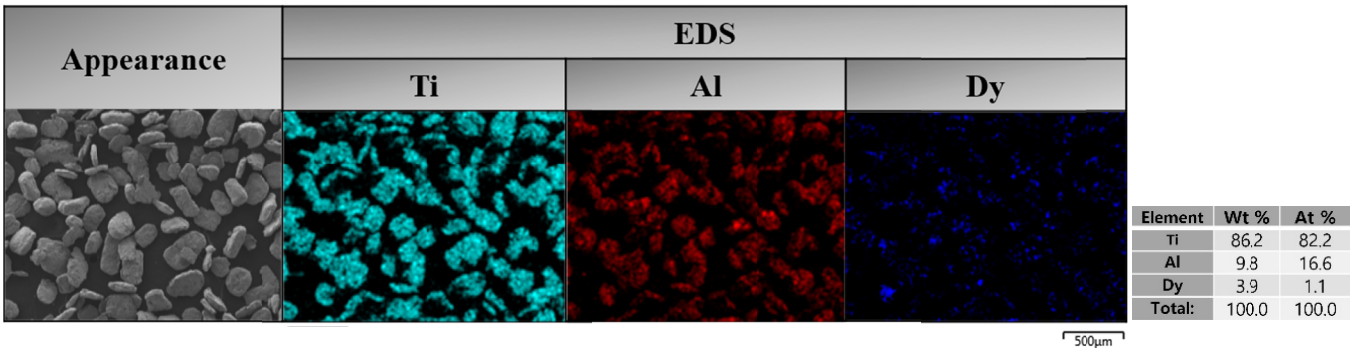

Fig. 2. EDS analysis of mixing powders milled at 600 rpm

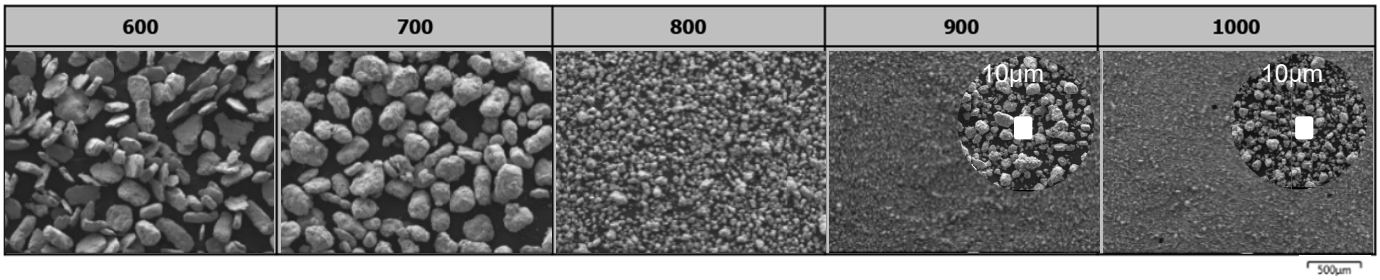

Fig. 3. SEM images showing Ti-Al-Dy mixing powders milled at 600 ~ 1000 rpm

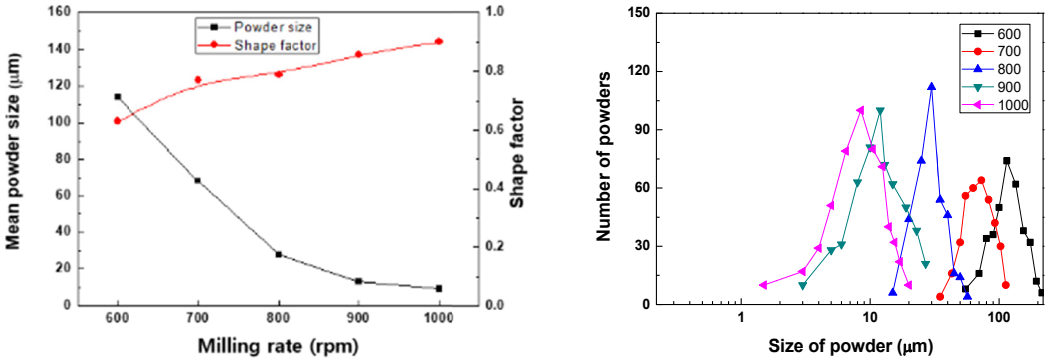

(a) (b)

Fig. 4. (a) Mean powder size, shape factor and (b) size distribution of as milled powders

Figure 5 shows XRD patterns of Ti-Al-Dy mixing powders milled at various milling rates of 600 ~ 1000 rpm. As the milling rate increases, the main peaks become broader, which indicates the continuous decrease of particle size. In addition, newly appeared peaks are detected at the milling rates of 800 ~ 1000 rpm. The peaks are analyzed as Ti_3Al and AlDy compounds, indicating that the mechanical alloying occurs by high energy ball milling at higher milling rate than 700 rpm.

The typical SEM image and EDS analysis of as sintered sample are shown in Fig. 6, along with a photograph of as sintered sample with a disc shape of 8mm in diameter and 4.1 mm in thickness. There are no observable cracks in the appearance of as sintered sample. The sintered sample reveals fully densified microstructure without any pores and approximately 99% in relative density, which results from the fact that the powders are sintered by joule heat occurring from spark plasma generated in the gap between powders for a short holding time at relatively low temperature. This indicates that sufficient substance migration including diffusion have occurred during SPS [21]. In addition, there are still very fine grains due to the rapid densification process which has the potential to minimize grain

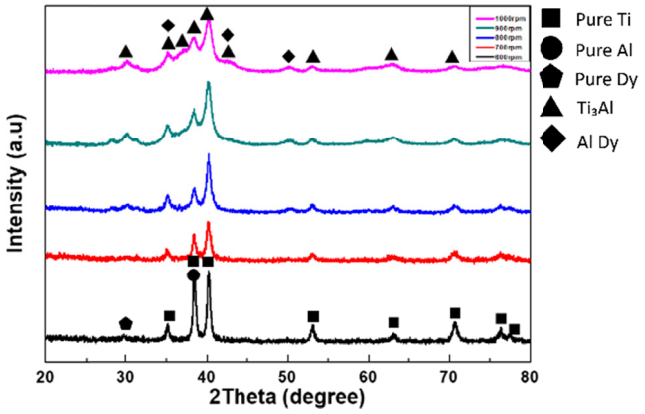

Fig. 5. XRD patterns of as milled powders

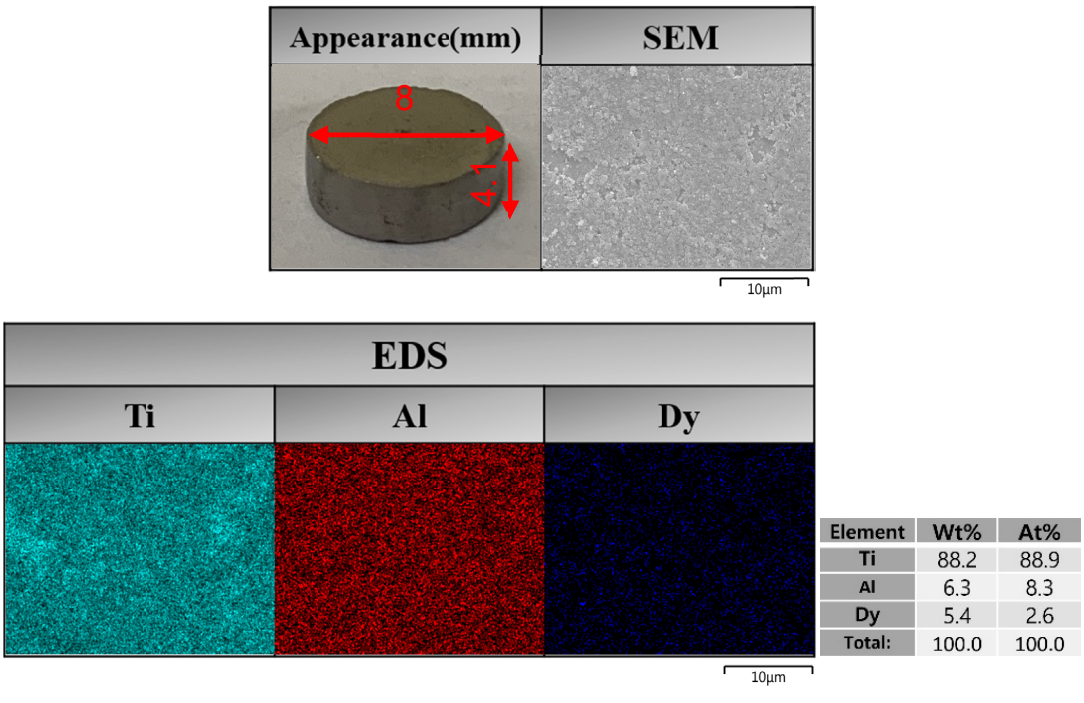

Element	Wt%	At%
Ti	88.2	88.9
Al	6.3	8.3
Dy	5.4	2.6
Total:	100.0	100.0

Fig. 6. SEM image and EDS analysis of as sintered sample

growth including second phases by enhancing sinterbility. From the EDS analysis, it is analyzed that the sintered sample contains the well-distributed 88.2wt%Ti, 6.3wt%Al and 5.4wt%Dy elements unlike the mixing powders shown in Fig.2, which well corresponds to the objective composition.

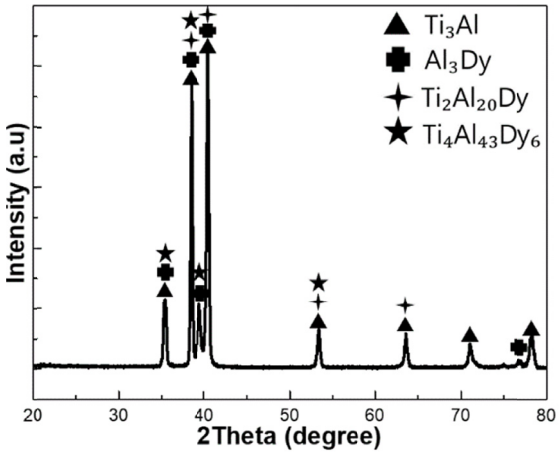

Fig. 7. XRD patterns of as sintered sample

Figure 7 shows the XRD patterns of as sintered sample. After SPS at 1373K, the peaks of AlDy phase shown in as milled powders disappeared, while the peaks of not only Ti_3Al but Al_3Dy were detected, which is generally considered to be due to the effective transfer of joule heat occurring from spark plasma. In the Ti-Al binary system, in general, there exist four intermetallic compounds such as Ti_3Al, TiAl, $TiAl_2$ and $TiAl_3$ at 773K [22]. In addition, it has been known that five intermetallic compounds of Al_3Dy, Al_2Dy, AlDy, Al_2Dy_3 and $AlDy_2$ are in the Al-Dy system while no intermetallic phase is found in the Ti-Dy binary system [22]. Niemann et al. [23,24] have reported that two ternary compounds of $DyTi_2Al_{20}$ and $Dy_6Ti_4Al_{43}$ were identified in the Ti-Al-Dy ternary system. Accordingly, in this study, two ternary $DyTi_2Al_{20}$ and $Dy_6Ti_4Al_{43}$ phases might exist as revealed in Fig. 7. Consequently, it is reasonably understood that the formation of Ti_3Al and AlDy phases during high energy ball milling might occur, and the Al_3Dy and two ternary $DyTi_2Al_{20}$ and $Dy_6Ti_4Al_{43}$ phases could be also formed by SPS. The size of second phases calculated by Debye-Scherrer's equation using the half-value width of XRD peaks is 15 ~ 60 nm.

On the other hand, the SPSed Ti-Al-Dy alloy reveals micro-hardness of more than 950 Hv, which is much higher than the commercial Ti-6Al-4V alloy with approximately 350 Hv in micro-hardness [25]. In general, for materials containing such second phases, the amount and nature of interface between matrix and second phases have a sensitive influence on the mechanical properties because these depend on the capability to transfer the stress through the interface. In particular, solute segregation and enhanced dislocation density can often facilitate nucleation of imperfections such as debonding and crack at the interface [26]. Nevertheless, we have recently reported that there were no noticeable debonding and pores at the interface between matrix and reinforcements for TiC reinforced Ti matrix composite by mechanical alloying and SPS [27], indicating that the Ti-Al-Dy alloy in this study might have good bonding between matrix and second phases. Accordingly, it is reasonably considered that much higher micro-hardness in the Ti-Al-Dy alloy is due to not only the fine and dense microstructure but nano sized second phases with good bonding at the interface between matrix and second phases after SPS.

4. Conclusions

The high energy ball milling was carried out for the alloying of Ti, 6wt%Al and 4wt%Dy powders at various milling rates of 600 ~ 1000 rpm for 3h under Ar atmosphere. As the milling rate increased from 600 to 1000 rpm, the size of mixing powders reduced from 120 to 15 μm. The peaks of Ti_3Al and AlDy phases in powders milled at higher speeds than 700 rpm were detected, indicating the occurrence of mechanical alloying. The Ti-Al-Dy powders milled at 800 rpm were subject to the SPS under the condition of 50 MPa in applied pressure at 1373K for 15 min. The AlDy phase completely disappeared after SPS, while the Al_3Dy and two ternary Ti-Al-Dy phases were formed. The SPSed Ti-6Al-4Dy alloy showed the dense and fine microstructure, resulting in approximately 99% in relative density. In addition, considering the commercial Ti-6Al-4V alloy showing approximately 350 Hv in micro-hardness, the SPSed Ti-6Al-4Dy alloy revealed much higher micro-hardness of more than 950Hv.

Acknowledgements

This work was supported by the Ministry of Trade, Industry and Energy (MOTIE, Korea) under Industrial Technology Innovation Program, No. 20000970.

REFERENCES

[1] M. Selva Kumar, P. Chandrasekar, P. Chandramohan, M. Mohanraj, Mater. Charact. **73**, 43-51 (2012).

[2] T. Matsuo, T. Nozaki, T. Asai, S.Y. Chang, M. Takeyama, Intermetallics **6**, 695-698 (1998).

[3] K. Kondoh, T. Threrujirapapomg, J. Umeda, B. Fugetsu, Compos. Sci. Tech. **72**, 1291-1297 (2012).

[4] F. Petzoldt, V. Friederici, P. Imgrumd, C. Aumund-Kopp, J. Korea Powder Metall. Inst. **21**, 1-6 (2014).

[5] Y. Song, D.S. Xu, R. Yang, D. Li, W.T. Wu, Z.X. Guo, Mater. Sci. and Eng. A **A260**, 269-274 (1999).

[6] T. Kawabata, T. Tamura, O. Izumi, Metall. Trans. **24A**, 141-150 (1993).

[7] S.M. Park, S.W. Nam, J.Y. Cho, S.H. Lee, S.G. Hyun, T.S. Kim, Arch. Metall. Mater. **65**, 1281-1285 (2020).

[8] S.W. Nam, R.M. Zarar, S.M. Park, S.H. Lee, S.G. D.H. Kim, T.S. Kim Arch. Metall. Mater. **65**, 1273-1276 (2020).

[9] S.M. Hong, E.K. Park, K.Y. Kim, J.J. Park, M.K. Lee, C.K. Rhee, J.K. Lee, Y.S. Kwon, J. Kor. Powd. Met. Inst. **19**, 32-39 (2012).
[10] H.P. Klug, L.E. Alexander, John Wiley and Sons, X-ray Diffraction Procedures for Polycrystalline and Amorphous Materials, New York 1997.
[11] S.J. Park, Y.S. Song, K.S. Nam, S.Y. Chang, J. Kor. Powd. Met. Inst. **19**, 122-126 (2012).
[12] S.Y. Chang, B.S. Kim, Y.S. Song, K.S. Nam, J. Nanosci. and Nanotech. **12**, 1353-1356 (2012).
[13] B.S. Kim, D.H. Lee, S.Y. Chang, Modern Physics Letters B **23**, 3919-3923 (2009).
[14] T. Takeuchi, M. Tabuchi, H. Kageyama, Y. Suyama, J. Am. Ceram. Soc. **82**, 939-943 (1999).
[15] Z.J. Shen, M. Johnson, Z. Zhao, M. Nygren, J. Am. Ceram. Soc. **85**, 1921-1927 (2002).
[16] G.D. Zhan, J.D. Kuntz, J.L. Wan, A.K. Mukherjee, Nat. Mat. **2**, 38-42 (2003).
[17] J.Y. Suh, Y.S. Song, S. Y. Chang, Arch. Metall. Mater. **64**, 567-571 (2019).
[18] S.Y. Chang, S.T. Oh, M.J. Suk, C.S. Hong, J. Kor. Powd. Met. Inst. **21**, 97-101 (2014).
[19] L. Gao, H. Miyamoto, J. Inorg. Mater. **12**, 129-133 (1997).
[20] M. Tokita, J. Soc. Powder Technol. **30**, 790-804 (1993).
[21] D.J. Kim et al., Korean Powder Metallurgy Inst, Powder Metallurgy & Particulate Materials Processing, Seoul 2010.
[22] H. Zhou, W. Liu, S. Yuan, J. Yan, J. Alloys and Comp. **336**, 218-221 (2002).
[23] S. Niemann, W. Jeitschko, J. Solid State Chem. **114**, 337-341 (1995).
[24] S. Niemann, W. Jeitschko, J. Solid State Chem. **116**, 131-135 (1995).
[25] http://asm.matweb.com/search/SpecificMaterial.asp?bassnum=MTP641.
[26] S.Y. Chang, S.J. Cho, S.K. Hong, D.H. Shin, J. Alloys and Comp. **316**, 275-279 (2001).
[27] W.H. Lee, J.G. Seong, Y.H. Yoon, C.H. Jeong, C.J. Van Tyne, H.G. Lee, S.Y. Chang, Ceramics Inter. **45**, 8108-8114 (2019).